Age-related changes in “cortical” 1/f dynamics are linked to cardiac activity

Fabian Schmidt[1]*, Sarah K. Danböck[1], Eugen Trinka[1,2,3], Gianpaolo Demarchi[1], Nathan Weisz[1,2]

[1]Paris-Lodron-University of Salzburg, Department of Psychology, Centre for Cognitive Neuroscience, Salzburg, Austria

[2]Neuroscience Institute, Christian Doppler University Hospital, Paracelsus Medical University, Salzburg, Austria

[3]Department of Neurology, Christian Doppler University Hospital, Paracelsus Medical University, Salzburg, Austria

ABSTRACT

The power of electrophysiologically measured cortical activity decays $1/f^{X}$. The slope of this decay (i.e. the spectral exponent) is modulated by various factors such as age, cognitive states or psychiatric/neurological disorders. Interestingly, a mostly parallel line of research has also uncovered similar effects for the spectral slope in the electrocardiogram (ECG). This raises the question whether these bodywide changes in spectral slopes are (in-)dependent. Focusing on well-established age-related changes in spectral slopes we analyzed a total of 1282 recordings of magnetoencephalography (MEG) resting state measurements with concurrent ECG in an age-diverse sample. We show that the aperiodic signal recorded using surface electrodes/sensors originates from multiple physiological sources. In particular, significant parts of age-related changes in aperiodic activity normally interpreted to be of neural origin can be explained by cardiac activity. Moreover, our results suggest that changes (flattening/steepening) of the spectral slope with age are dependent on the recording site and investigated frequency range. Our results highlight the complexity of aperiodic activity while raising concerns when interpreting aperiodic activity as “cortical“ without considering physiological influences.

INTRODUCTION

Aperiodic neural activity is omnipresent both in invasive (e.g. ECoG (Miller et al., 2009)) and non-invasive (e.g. MEG/EEG (Demanuele et al., 2007; Pritchard, 1992)) recordings of electrophysiological brain activity and even in hemodynamic responses (e.g. fMRI (B. J. He et al., 2010)). In the frequency domain, when visualized in log-log coordinates (log-frequency/log-power), aperiodic activity manifests as a linear decay in power with an increase in frequency (Miller et al., 2009). This part of the signal - following a so-called "power-law" distribution - is often referred to as "scale-free", "1/f noise" or more recently "aperiodic neural activity" (Donoghue et al., 2020).

In the past, aperiodic neural activity, other than periodic neural activity (local peaks that rise above the "power-law" distribution), was often treated as noise and simply removed from the signal e.g. via pre-whitening (Buzsáki, 2006; Mitra & Pesaran, 1999). However, in recent years the analysis of aperiodic neural activity has gained interest. Several studies have shown that aperiodic neural activity is meaningfully modulated by various factors, such as age (Voytek et al., 2015), cognitive state (e.g. awake vs. sleep; (B. J. He et al., 2010)) and disorders like Parkinson's disease and epilepsy (Ghinda et al., 2021; Mostile et al., 2019). However, aperiodic activity is not only present in recordings of neural activity, but also part of other physiological signals such as cardiac and muscle activity, commonly measured using electrocardiography (ECG; (Saul et al., 1988)) and electromyography (EMG; (Kozhemiako et al., 2022)). Interestingly, and mostly overlooked by the neuroscience community, aperiodic activity measured using ECG has also been linked to aging (Beckers et al., 2006), different cognitive states (eg. awake vs. sleep; (Kozhemiako et al., 2022; Penzel et al., 2003)) and disorders such as Parkinson's disease and epilepsy (Ansakorpi, 2002; Haapaniemi, 2001).

It is well known that, via volume conduction, cardiac activity can also be captured in invasive and non-invasive recordings of neural activity (Dirlich et al., 1997; Jousmäki & Hari, 1996; Kern et al., 2013). In MEG recordings cardiac activity is routinely measured via ECG and commonly rejected from the signal (Gross et al., 2013). In clinical EEG recordings, e.g. for the diagnosis of epilepsy, the recording of ECG is standard practice. However, in cognitive neuroscience research the influence of cardiac activity on the EEG is often deemed less problematic (Dirlich et al., 1997) and ECG is rarely recorded/reported. This may be problematic as ECG signals recorded at the head can reach amplitudes of ~5-15μV, which is on par with the size of common evoked responses measured using EEG

(Haenschel et al., 2007; von Rosenberg et al., 2017).

Given that aperiodic activity in recordings of neural and cardiac activity is modulated by similar traits, states and disorders, we ask: are these bodywide changes in aperiodic activity (in-)dependent? To address this question, we turn our attention to the recently reported (Donoghue et al., 2020; Voytek et al., 2015) and replicated (Merkin et al., 2022) association between aperiodic activity and chronological age. Using the publicly available Cam-CAN dataset (Shafto et al., 2014; Taylor et al., 2017), we find that the aperiodic signal recorded using surface electrodes originates from multiple physiological sources. In particular, significant parts of age-related changes in aperiodic activity normally interpreted to be of neural origin can be explained by cardiac activity. Furthermore, the impact of cardiac and neural age-related changes in aperiodic activity varies depending on the frequency range and recording site. Our results highlight the complexity of aperiodic activity while raising concerns when interpreting aperiodic activity as “neural“ without considering physiological influences.

RESULTS

Aperiodic signals recorded using ECG are associated with aging

Changes of aperiodic activity in recordings of neural and cardiac activity are associated with aging (Beckers et al., 2006; Voytek et al., 2015). However, analyses of ECG signals - in the frequency domain - typically focus on (a-)periodic signals <0.4Hz (Shaffer & Ginsberg, 2017). These (compared to neural time series) slowly fluctuating signals are related to heart rate variability (Task Force of the European Society of Cardiology the North American Society of Pacing Electrophysiology, 1996). Changes in (a-)periodic activity at these low frequencies are well established physiological measures (Azuaje et al., 2006). While meaningful information of the ECG can be extracted at much higher rates (e.g. ventricular late potentials [80-500Hz]; (Hunt, 2002)) substantially less is known about aperiodic activity above 0.4Hz in the ECG. To understand whether aperiodic activity recorded using ECG carries meaningful information about aging - at frequency ranges common in M/EEG recordings - the ECG data of 4 age-diverse populations with a total of 2286 subjects were analyzed.

After pre-processing (see Methods), age was used to predict the spectral slope of the ECG.

Our results show that the association between age and the spectral slope increased with the frequency range used to estimate the spectral slope up to ~145 Hz (see Figure 1C). Due to the presence of a “knee” in the ECG data (for details regarding “knees” in power spectra see (Donoghue et al., 2020; Gao et al., 2020; Miller et al., 2009)), slopes were fitted individually to each subject's power spectrum in log-log space (see Figure 1B for the distribution of knee frequencies across datasets). At a frequency range of ~15-145 Hz, age correlated positively with the spectral slope measured using ECG indicating an age-related flattening in Dataset 1 (r = .22, *HDI*=[.15, .29]), Dataset 2 (r = .39, *HDI*=[.32, .46]), Dataset 3 (r = .23, *HDI*=[.15, .29]) and Dataset 4 (r = .27, *HDI*=[.20, .34]; see Figure 1D). These results show that aperiodic activity measured via ECG is associated with aging at frequency ranges vastly exceeding those typically investigated via ECG, but overlapping with frequency ranges commonly measured in recordings of neural activity (see Figure 1BC). Importantly, the direction of the association between age and aperiodic ECG activity is identical to that reported for age and aperiodic EEG activity (Donoghue et al., 2020; Voytek et al., 2015), motivating the investigation of these relationships in combined neural and cardiac measurements.

Cardiac activity is directly captured in EEG and MEG recordings

Aperiodic activity recorded using ECG (see Figure 1A) and EEG/ECoG (Voytek et al., 2015) is similarly modulated by age. In most MEG and some EEG recordings cardiac activity is measured via ECG (Gross et al., 2013). Components of the signal related to cardiac activity are then commonly removed (e.g. via ICA (Hyvarinen, 1999)). In recordings of EEG the influence of cardiac activity is often deemed less problematic (Dirlich et al., 1997), as a result ECG is rarely recorded. However, this may be problematic as ECG signals recorded at the head can reach amplitudes of ~5-15μV, which overlap with the amplitude of evoked responses measured using EEG (Haenschel et al., 2007; von Rosenberg et al., 2017) and may therefore also be present in measurements of neural activity.

We utilized concurrent ECG, EEG and MEG resting state recordings to examine to what extent ECG signals are present in the signals measured using MEG and EEG. We calculated so-called temporal response functions (see Methods), to detect whether the signals recorded at different locations (M/EEG vs. ECG) are instantaneously related (zero-time-lags; and therefore likely correspond to the same source) or if one lags behind the other (non

zero-time-lags; likely different sources influencing each other e.g. via interoception see (Schulz, 2016)). After pre-processing (see Methods) the data was split in three conditions using an independent component analysis (ICA; (Hyvarinen, 1999)). Independent components that were correlated (at $r > 0.4$; see Methods) with the ECG electrode were either not removed from the data (Figure 1EFGH - blue), removed from the data (Figure 1EFGH - orange) or projected back separately (Figure 1EFGH - green). Afterwards, temporal response functions (encoding models; see Methods) between the signal recorded at the ECG electrode and the MEG/EEG sensors and feature reconstruction models (decoding models) were computed (for each condition respectively). Our results show that if ECG components are not removed via ICA the ECG signal is captured equally strong at zero-time-lags both in EEG and MEG recordings (see Figure 1EGH). Even after removing ECG related components from the data TRF peaks emerged (although reduced) at zero-time-lags in EEG, but not in MEG recordings (see Figure 1EF). Furthermore, reconstruction (decoding) of the ECG signal was reduced, but remained above chance even after rejecting the ICA signal using ECG both in MEG and EEG recordings ($r > 0$). Interestingly, the presence of the ECG signal was more pronounced in EEG compared to MEG recordings, after removing ECG related components ($\beta_{standardized\ (EEG > MEG)} = 0.97$, $HDI = [0.42, 1.52]$; Figure 1H). Additionally, ECG related components extracted from MEG recordings were more related to the ECG signal than the components extracted from the EEG ($\beta_{standardized\ (EEG > MEG)} = -0.76$, $HDI = [-1.35, -0.18]$; Figure 1H). These results show that a) residual ECG activity remains in surface neural recordings, even after applying a very sensitive threshold to detect and remove ECG components via ICA and b) neural and cardiac activity are more difficult to separate in EEG as opposed to MEG recordings (see Figure 1EGH) resulting in more residual (after ICA) ECG related activity in EEG recordings.

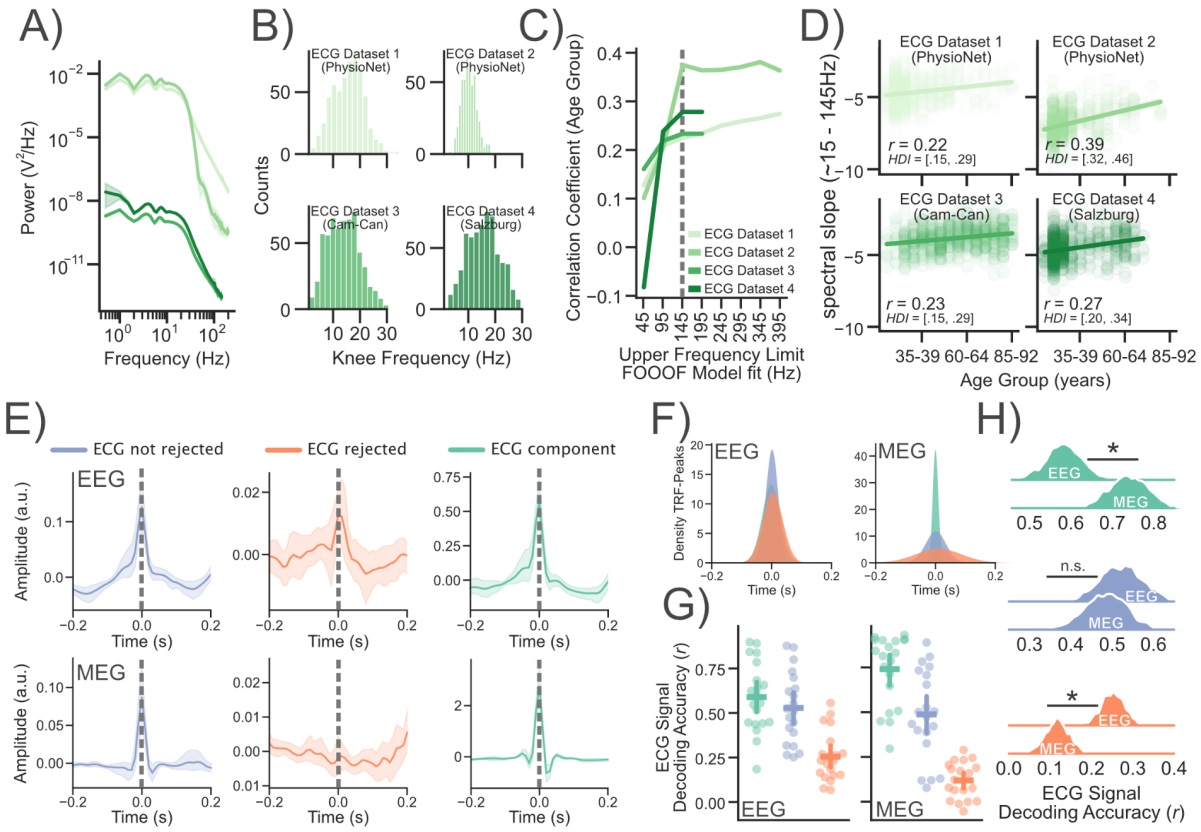

Figure 1: Aperiodic signals recorded using ECG can be associated with aging **(ABCD)**. Cardiac activity is captured in EEG and MEG recordings **(EFGH)**. **A)** grand average power spectra plotted separately per Dataset **B)** indicating a strong "knee" from ~15Hz**. CD)** The spectral slope recorded using ECG was calculated using different upper frequency limits and correlated with age. This analysis shows that the association between age and spectral slope increased until ~145 Hz in 3 of 4 datasets. **EF)** Cardiac activity is captured at zero time lags in concurrent MEG and EEG recordings, if the ECG signal is rejected via ICA this effect disappears in MEG, but not completely in EEG data. **GH)** Reconstruction of the ECG signal was impaired, but remained possible even after rejecting the ICA signal using ECG (both in MEG and EEG data). Notably, reconstruction of the ECG signal (after ICA) worked better in EEG than MEG data. A * indicates a "significant" effect (see Methods - Statistical Inference).

Age-related changes in aperiodic brain activity across sensors are most pronounced in cardiac components

ECG signals are captured in brain activity recorded using M/EEG (see Figure 1EFGH). Furthermore, aperiodic activity recorded using ECG is - just like aperiodic activity recorded using EEG/ECoG - modulated by age (see Figure 1CD). However, it is unclear whether these bodywide changes in aperiodic activity are (in-)dependent.

To answer this question we are leveraging resting state MEG recordings of an age-diverse

population obtained from the Cam-CAN inventory (N = 627; (Shafto et al., 2014; Taylor et al., 2017). After pre-processing (see Methods) an ICA was applied to separate MEG activity from activity related to the ECG. ICA components that were related to the ECG signal were identified using a threshold ($r > 0.4$; same threshold as in 1EFGH). The data was split into three conditions ($MEG_{ECG\ not\ rejected}$ [blue], $MEG_{ECG\ rejected}$ [orange] and $MEG_{ECG\ component}$ [green]; see Figure 2A) and projected back to the sensor space respectively. Age was then used to predict the spectral slope averaged across all 102 magnetometers per subject (split by condition). The results show that the spectral slope steepens with age when the ECG signal is not rejected (Figure 2A - blue; $\beta_{standardized}$ = -0.17, HDI = [-0.24, 0.10]). Rejecting the ECG signal (Figure 2A - orange) weakens the "steepening effect" of age on the spectral slope ($\beta_{standardized}$ = -0.09, HDI = [-0.17, -0.02]). The strongest effect of age on the spectral slope was found in the data reflecting only the ECG components (green; $\beta_{standardized}$ = -0.32, HDI = [-0.39, -0.25]). These results show that the relationship between age and the broadband spectral slope (0.1-145Hz; for a median split age comparison of raw power spectra see Supplementary 1A), averaged across all MEG sensors, is most pronounced on the ICA components related to the ECG extracted from the MEG data. We further repeated this analysis by fitting slopes on the broadband aperiodic spectrum extracted using IRASA across different frequency ranges with lower limits starting at 0.5 Hz in 1 Hz steps ranging until 10 Hz and upper limits starting at 45 Hz in 5 Hz steps ranging until 145 Hz (see Figure 2B). The results of this analysis show that the spectral slope averaged across MEG sensors steepens with age across a wide range of slope fitting options. However, this steepening effect was largely only significant in the data reflecting solely the ECG components (see Figure 2B). On the $MEG_{ECG\ not\ rejected}$ and $MEG_{ECG\ rejected}$ data significant steepening effects were only observed for specific frequency ranges. The strength of the age-related steepening effect further varied depending on whether or not a Signal-Space-Separation algorithm (SSS; (Taulu & Kajola, 2005; Taulu & Simola, 2006)) was applied to the data prior to the analysis (see Supplementary S4). Slightly stronger steepening effects were observed for the $MEG_{ECG\ not\ rejected}$ data compared to $MEG_{ECG\ rejected}$ when not cleaning the data using SSS (see Figure 2A) and vice versa (see Supplementary S4). To ensure that the effects shown are not dependent on the ICA thresholds used, the analysis in 2A was also conducted for other thresholds showing a similar pattern (see Supplementary S5). We further managed to replicate the finding that age has the strongest impact on the spectral slope of the ECG components using a different algorithm to extract aperiodic activity

(FOOOF; (Donoghue et al., 2020); see Supplementary S2) and on an additional dataset containing resting state recordings (*N* = 655) obtained as part of MEG studies routinely conducted at the University of Salzburg (see Supplementary S3). Surprisingly, all these results indicate an age-related steepening in the spectral slope of MEG data averaged across sensors. This finding is contrary to previous findings showing a flattening of spectral slopes with age in recordings of brain activity (Voytek et al., 2015) and cardiac activity (Beckers et al., 2006; see also Figure 1CD). This discrepancy can potentially be explained by multiple factors including, physiologically measured 1/f noise differently affecting magnetic and electric recording devices (e.g. see Dehghani et al., 2010), preprocessing choices, fitting ranges for the 1/f slope, electrode selection etc. (see discussion).

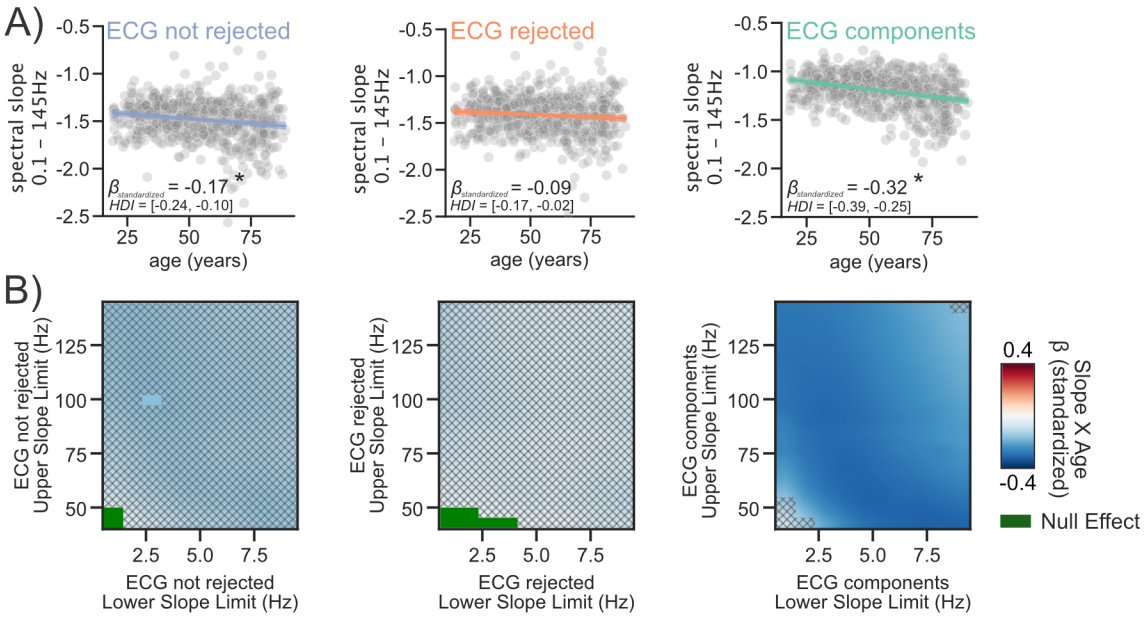

Figure 2: Age-related changes in aperiodic brain activity across sensors are most pronounced in cardiac components **A)** Age was used to predict the spectral slope (fitted at 0.1-145Hz) at rest in three different conditions (ECG components not rejected [blue], ECG components rejected [orange], ECG components only [green]. A * indicates a significant effect (see Methods - Statistical Inference). **B)** The analysis in **A)** was repeated for different fitting ranges with lower limits starting at 0.5 Hz in 1Hz steps ranging until 10 Hz and upper limits starting at 45 Hz in 5 Hz steps ranging until 145 Hz. Significant effects, i.e. effects with credible intervals not overlapping with a region of practical equivalence (ROPE; see Methods - Statistical Inference), are highlighted in red or blue (see colorbar). Null effects, which were defined as effects with credible intervals completely within a ROPE, are highlighted in green. Results where no decision to accept or reject (see (Kruschke, 2018)) an effect could be made, are masked using hatches.

Changes (steepening/flattening) of the spectral slope with age are dependent on the recording site and the investigated frequency range

Our results show - in contrast to previous findings - a steepening in the spectral slope extracted from the MEG with age. This effect is most pronounced in components related to the ECG (see Figure 2), robust across two large MEG datasets (see Supplementary S3) and different processing options (see Supplementary S2, S4, S5). However, as we ran this analysis on the average across channels, possible differences at subsets of channels were ignored. We therefore repeated the analysis above on single MEG channels (see Figure 3). To investigate potential age-related local changes in aperiodic activity.

This analysis shows that over a broad amount of individual fitting ranges and channels, aging resulted in a steepening of spectral slopes across conditions (see Figure 3E) with "steepening effects" observed in 25% of the processing options in $MEG_{ECG\ not\ rejected}$, 0.5% in $MEG_{ECG\ rejected}$, and 60% for $MEG_{ECG\ components}$. The second largest cluster of effects were "null effects" in 13% of the options for $MEG_{ECG\ not\ rejected}$, 30% in $MEG_{ECG\ rejected}$, and 7% for $MEG_{ECG\ components}$. However, we also found "flattening effects" in the spectral slope for 0.16% of the processing options in $MEG_{ECG\ not\ rejected}$, 0.3% in $MEG_{ECG\ rejected}$, and 0.46% in $MEG_{ECG\ components}$. The age-related flattening in spectral slopes occurred mainly at centrally and parietally located electrodes in lower frequency ranges between 0.5 and 45Hz (see Figure 3C). Importantly, these results overlap both in frequency range and recording site with those previously reported in the literature (e.g. see (Tröndle et al., 2022; Voytek et al., 2015)). A majority of results fall in the category "undecided" (see Figure 3EFG) as there was not enough evidence to either support a steepening, flattening or null effect (see (Kruschke, 2018)). Albeit undecided we still visualized the respective direction of these results labeling them either as "undecided/steepening" or "undecided/flattening" to give a descriptive overview of the associated spatial locations and frequency ranges in which these results were observed (see Figure 3EF). In sum, this analysis suggests that a flattening of spectral slopes with age can be observed at previously reported frequency ranges (~0.5-45Hz) and spatial locations (on central, parietal and occipital sensors). However, these results represented only 0.3% of effects across all processing settings (conditions, sensors and frequency ranges). Even when restrictively looking only at all the investigated frequency ranges between 0.5 and 50Hz, only 1.2% (0.4% after maxfilter see Supplementary S6) of

effects across these residual settings were showing an age related flattening of the spectral slope. This suggests that age-related flattening of the spectral slope is tied to specific recording sites and frequency ranges. A vast majority of effects we observed show a steepening of the spectral slope with age across sensors and frequency ranges. The topography of these observed steepening effects is present across the scalp and prominent at frontal and temporal sensors around the MEG helmet (albeit also observable at central locations; see $MEG_{ECG\ Components}$). This topography is suggestive of artifacts induced by muscle activity (e.g. head/eye movements). We therefore used the subject's head movement information obtained via continuous hpi measurements as a covariate (i.e. 5 coils continuously emitting sinusoidal waves at 293 Hz, 307 Hz, 314 Hz, 321 Hz and 328 Hz to localize the head position in the scanner). While head movements increased significantly with aging ($\beta_{standardized}$ = 0.23, *HDI* = [0.28, 0.18], see Supplementary S7) it was not sufficient to explain the observed steepening or flattening effects in the spectral slope (see Supplementary S7). We further investigated age-related changes to the spectral slope of the vertical and horizontal EOG channels indicating no significant age-related steepening/flattening across the investigated frequency ranges (see Supplementary S7).

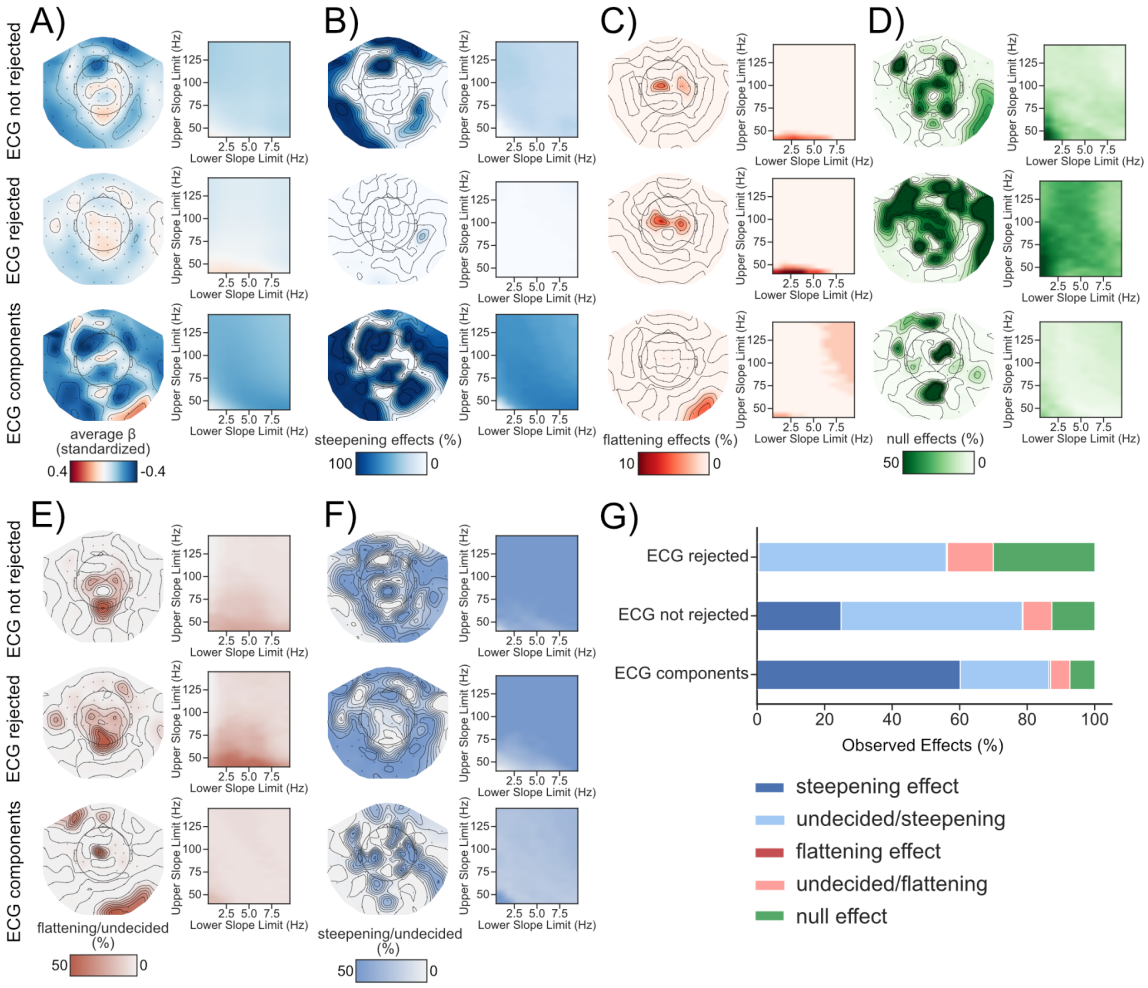

Figure 3: Steepening and flattening of the spectral slope with age is dependent on the recording site and the investigated frequency range. Age was used to predict the spectral slope at rest in three different conditions (ECG components not rejected, ECG components rejected and ECG components only) per channel across a variety of frequency ranges (see Figure **1B**). **A)** Standardized beta coefficients either per channel averaged across all frequency ranges (left) or per frequency range (right) averaged across all channels. Age-related **B)** steepening, **C)** flattening and **D)** null effects in the spectral slope were observed and visualized in a similar manner as in **A)**. **EF)** We further show the direction of results where we didn't find enough evidence to support either a steepening, flattening or null effect. **G)** Summary of all observed findings in %.

Age-related changes in aperiodic brain activity are linked to cardiac activity in a frequency dependent manner

So far we have shown that age-related steepening/flattening of the spectral slope in the MEG is both dependent on the investigated frequency range and the sensor selection. While a vast majority of our results indicate an age-related steepening of the spectral slope

(in contrast to previous findings), we also noted a flattening of the spectral slope at a subset of central sensors in the lower frequency range (~0.5-45Hz; in line with previous findings; (Tröndle et al., 2022; Voytek et al., 2015)). Some of the observed age-related flattening and steepening effects were solely present in one of the tested conditions (see Figure 4A). This suggests that aperiodic brain activity ($MEG_{ECG\ rejected}$), at some frequency ranges, changes with age independently of cardiac activity ($MEG_{ECG\ component}$) and vice versa. However, we also noted shared effects at other frequency ranges (i.e. effects present both in the $MEG_{ECG\ rejected}$ and $MEG_{ECG\ component}$ condition; see Figure 4B). To see if $MEG_{ECG\ rejected}$ and $MEG_{ECG\ component}$ explain unique variance in aging at frequency ranges where we noticed shared effects, we averaged the spectral slope across significant channels and calculated a multiple regression model with $MEG_{ECG\ component}$ and $MEG_{ECG\ rejected}$ as predictors for age. This analysis reveals that when adding both $MEG_{ECG\ component}$ and $MEG_{ECG\ rejected}$ as predictors age-related flattening effects were reduced, yielding no longer significant flattening results (see Figure 4B; upper panel). However, in case of the observed steepening effects, significant effects for $MEG_{ECG\ components}$ remained in 98.75% of the tested frequency ranges (see Figure 4B; lower panel). In sum, these results suggest that whether or not aperiodic brain activity changes independently from cardiac activity with age depends on the recording site and the selected frequency range.

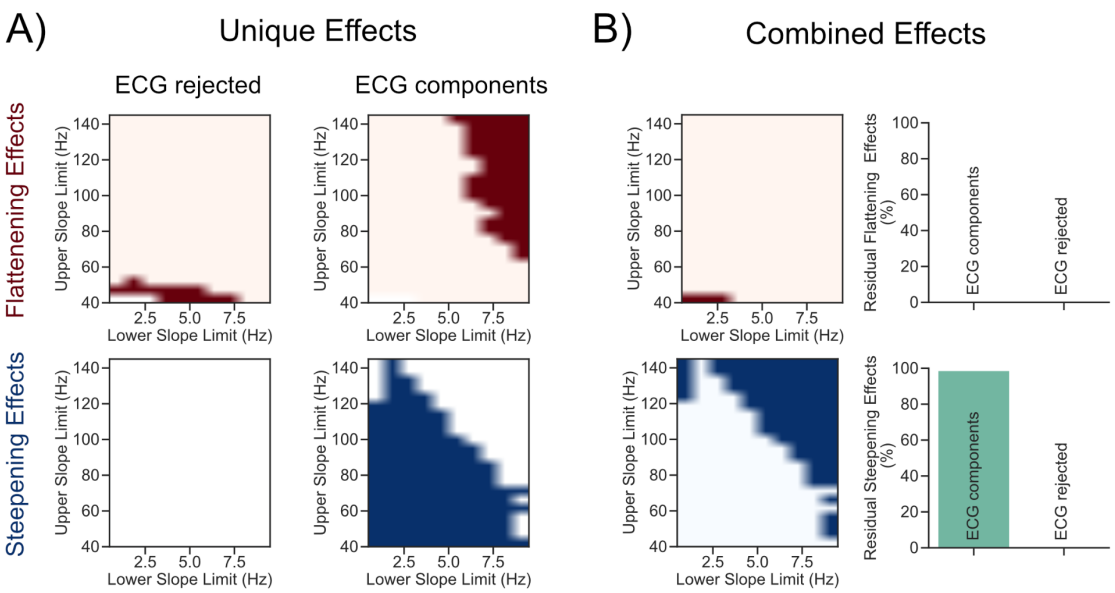

Figure 4: Age-related changes in aperiodic brain activity are linked to cardiac activity in a frequency dependent manner. **A)** At some frequency ranges neural and cardiac aperiodic activity change independently with age. **B)** At other frequency ranges cardiac and neural aperiodic activity are similarly modulated by age. We used cardiac and neural aperiodic activity as predictors for age in a multiple regression model to test whether both explain unique variance in aging. This analysis reveals that when adding both $MEG_{ECG\ component}$ and $MEG_{ECG\ rejected}$ as predictors age-related flattening effects were reduced, yielding no longer significant flattening results (see Figure 4B; upper panel). However, in case of the observed steepening effects, significant effects for $MEG_{ECG\ components}$ remained in 98.75% of the tested frequency ranges (see Figure 4B; lower panel).

DISCUSSION

Cardiac and cortical recordings of aperiodic electrophysiological signals are related to age (Beckers et al., 2006; Voytek et al., 2015), cognitive states (eg. awake vs. sleep; (B. J. He et al., 2010; Penzel et al., 2003)) and disorders such as Parkinson's disease and epilepsy (Ansakorpi, 2002; Ghinda et al., 2021; Haapaniemi, 2001; Mostile et al., 2019). In the present study we investigated whether age-related changes in neural and cardiac aperiodic activity are (in-)dependent. Our results suggest that the aperiodic signal recorded using surface sensors/electrodes originates from multiple physiological sources. In particular, significant parts of age-related changes in aperiodic activity normally interpreted to be of neural origin can be explained by cardiac activity.

Aperiodic processes are ubiquitous in nature (Gisiger, 2001). They can be observed not only in physiological recordings but are also found in earthquakes, economics, ecology,

epidemics, speech, and music (Bak et al., 1987; Gisiger, 2001). In measurements containing multiple aperiodic signals, aperiodic signals might even influence each other (e.g. neural speech tracking; (Chen et al., 2023; Schmidt et al., 2021)). Understanding the generative process underlying aperiodic signals is therefore crucial to correctly attribute functional changes in aperiodic activity to the right source.

Differences in aperiodic activity between magnetic and electric field recordings

Surprisingly, a vast amount of our results using MEG data indicate a steepening of the spectral slope with age. This is contrary to previous findings using mainly EEG/ECoG data (Voytek et al., 2015) that commonly show a widespread flattening of the spectral slope with age (e.g. see Voytek et al. 2015). Similarly, we also noticed an age-related flattening on simultaneous ECG recordings (see Figure 1CD). So do these discrepancies reflect general differences between electric vs. magnetic recordings of physiological activity? Previous research has shown scaling differences in the spectral slope between MEG and EEG recordings (Dehghani et al., 2010). These scaling differences are partly widespread (overall flatter sloped spectra in MEG data) and partly regionally-specific (steeper sloped spectra at vertex in MEG compared to EEG recordings and vice versa at frontal regions). These observations have been linked to non-resistive properties of tissue (i.e. the propagation of the electric field through tissue is frequency dependent; see (Bedard et al., 2017; Dehghani et al., 2010). This differently affects the signal recorded using MEG and EEG, as magnetic field recordings are not distorted by the tissue conductivity of the scalp, skull, cerebrospinal fluid and brain (Singh, 2014). An alternative, but not exclusive, hypothesis suggests that even under the assumption of a purely resistive medium (which is unlikely, see (Bedard et al., 2022; Gomes et al., 2016)), frequency scaling differences between MEG and EEG may emerge in relation to the space/frequency structure of the recorded activity (Bénar et al., 2019). Under this hypothesis lower frequencies are suggested to involve synchronous activity in larger patches of cortex whereas higher frequencies involve synchronous activity in smaller cortical patches. The authors demonstrate that EEG typically integrates activity over larger volumes than MEG, resulting in differently shaped spectra across both recording methods. During aging both changes in conductive tissue properties (e.g. (Mohammed et al., 2017; Thomas et al., 2018)) and functional connectivity occur (Deery et al., 2023). Hypothetically, an interaction between several factors that differently affect MEG and EEG (e.g. age-related changes in non-resistive properties of tissue and in functional connectivity)

may therefore potentially explain differently shaped spectra in MEG compared to EEG recordings.

Influences of preprocessing decisions on age-related changes in aperiodic activity

While differences between magnetic and electric field recordings may explain some observed differences in the widespread effects between electric and magnetic recordings of electrophysiological activity, we still observed flatter sloped spectra with age at a few MEG sensors across several frequency ranges (see Figure 3C, 4). These findings are also in-line with previous analyses of MEG data investigating age-related changes in aperiodic activity (He et al., 2019; Thuwal et al., 2021). The frequency dependence of the flattening/steepening effects (see Figure 3) suggests that the slope of the power spectrum can be very sensitive to different preprocessing decisions that may emphasize different aspects of (neuro-)physiological activity. In case of the MEG signal this may include the application of Signal-Space-Separation algorithms (SSS; (Taulu & Kajola, 2005; Taulu & Simola, 2006)), high and low pass filtering, choices during spectral density estimation (window length/type etc.), different parametrization algorithms (e.g. IRASA vs FOOOF) and selection of frequency ranges for the aperiodic slope estimation. We therefore applied a wide variety of processing settings when analyzing our data. Our results indicate overall steeper sloped spectra with increasing age across datasets and processing options for MEG. These observed steepening effects can be explained by cardiac activity (see Figure 4). Cardiac activity, in the form of the ECG, is also captured in EEG recordings (via volume conduction; see Figure 1EFGH). Our data suggests that the ECG signal is captured equally strong in concurrent MEG and EEG recordings (see Figure 1EFGH). Furthermore, separating ECG related components from neural activity using ICA seems to work worse in EEG compared to MEG recordings (see Figure 1EF). Difficulties in removing ECG related components from EEG signals via ICA might be attributable to referencing. A presence of the ECG signal on reference electrodes might lead to the presence of ECG signals across all EEG electrodes. This may make it more difficult to isolate independent ECG components. Previous work (Kozhemiako et al., 2022; Lendner et al., 2020) has shown that a linked mastoid reference was particularly effective in reducing the impact of ECG related activity on aperiodic activity measured using EEG. However, it should be considered that depending on the montage, referencing can induce ambiguities to the measured EEG signal. Linked mastoid referencing for instance can distort temporal activity (Feindel et al., 2009), which is unproblematic in studies focussing on activity on central electrodes (as in

(Kozhemiako et al., 2022; Lendner et al., 2020)), but should be considered when focusing on activity from other recording sites (for reference see (Yao et al., 2019)).

To better delineate cardiac and neural contributions when investigating aperiodic activity, ECG recordings should become more standard practice in EEG research. Additionally, further method development is needed to better separate cardiac from neural activity in M/EEG recordings.

(Neuro-)physiological origins of aperiodic activity

Aperiodic activity is present in recordings of different physiological signals, including neural (He et al., 2010), cardiac (Saul et al., 1988), and muscle activity (Kozhemiako et al., 2022). Our study investigated age-related changes in aperiodic activity using MEG, and found that these changes vary depending on the frequency range and recording site. Specifically, some changes were found to be uniquely linked to either cardiac or brain activity (Figure 4A), while others were present in both signals (Figure 4B). Interestingly, some of these shared effects could be attributed to cardiac activity (see Figure 4B; lower panel). However, some effects appeared to be equally influential in explaining age-related changes in both cardiac and brain activity, such that the individual effects disappeared when analyzed jointly (see Figure 4B, upper panel).

These findings underscore the complexity of analyzing aperiodic activity, indicating that the aperiodic signal recorded non-invasively originates from multiple physiological sources. These shared effects are particularly interesting, as they suggest that a common mechanism across physiological signals exists that underlies age-related changes of aperiodic activity. In fact, neural and vascular processes are known to interact with each other (Takarada-Iemata et al., 2019). Cardiovascular activity, in the form of the ECG, is also captured in M/EEG recordings (via volume conduction; see Figure 1CDEF). How longitudinal changes in neural and cardiac processes influence age-related changes in aperiodic activity is an exciting research question. This could be investigated in future studies utilizing longitudinal recordings of joint cardiac and neural activity. Understanding the relationship between neural and cardiac aperiodic activity is essential not only for identifying common underlying processes, but also for improving our understanding of the individual generative mechanisms of cardiac and neural aperiodic activity.

For example, a current popular hypothesis states that the generative process underlying aperiodic neural activity is mainly attributed to differences in the ratio between excitatory (AMPA) and inhibitory (GABA) currents, that influence the slope of the neural power

spectrum (Gao et al., 2017). Excitatory currents such as AMPA decay faster, then inhibitory currents like GABA. This means that flatter power spectra may be indicative for the presence of more excitatory than inhibitory currents and vice versa (steeper sloped power spectra; see (Gao et al., 2017)). This theory is (in part) based on research showing that GABAergic drugs like propofol (Gao et al., 2017) and Glutamatergic drugs like ketamine (Waschke et al., 2021) modulate the slope of electrophysiologically measured power spectra. However, propofol and ketamine not only influence neural activity, but also influence heart rate variability (a core component of the ECG; (Goddard et al., 2021; Kanaya et al., 2003)). So, are drug induced effects on the slope of the power spectrum (measured using surface electrodes) conflated by changes in cardiac activity? Previous work has shown that propofol induced changes to the spectral slope were still present in EEG recordings after using ICA to reject ECG components from the data (Lendner et al., 2020). However, our results suggest that cardiac activity remains in EEG signals even after doing an ICA with a very sensitive rejection criterion (see Figure 1EFGH). It is therefore plausible that drug induced effects on aperiodic “neural” activity can still be conflated by cardiac activity. Future work is needed to see to what extent drug induced changes in aperiodic neural activity can also be attributed to ECG signals. Similar caveats adhere to other findings of functional modulations in aperiodic signals in cognitive states (e.g. awake vs. sleep; (He et al., 2010; Penzel et al., 2003)) and disorders like Parkinson's disease and epilepsy (Ansakorpi, 2002; Ghinda et al., 2021; Haapaniemi, 2001; Mostile et al., 2019).

To conclude: The present study, focusing on age-related changes in aperiodic neural and cardiac activity indicates that the aperiodic signal recorded using surface sensors/electrodes originates from multiple physiological sources. The impact of cardiac and neural age-related changes in aperiodic activity varies depending on the frequency range and recording site. Conflating cardiac and neural contributions to aperiodic activity obstructs our understanding of both neural and cardiac aperiodic processes and should be avoided. These results highlight the need for concurrent recordings of cardiac and neural activity to further increase our understanding of aperiodic activity and its association with age, cognitive states, and disorders.

METHODS

Sample

The present study builds on resting-state data from several sources. ECG Datasets 1 & 2 were obtained from PhysioNet (Goldberger et al., 2000) containing 1121 healthy volunteers between 18 and 92 years of age (divided into 15 age groups for anonymization purposes) (Schumann & Bär, 2021). The MEG data analyzed in this study was obtained from two different sources: the Cam-CAN repository (main manuscript; (Shafto et al., 2014; Taylor et al., 2017)) and resting-state data routinely recorded at the University of Salzburg (Supplementary S3). The sample obtained from Cam-CAN contained 655 healthy volunteers with an age range between 18 and 88 years of age with an average age of 54 and a standard deviation of 18 years. The sample obtained from the University of Salzburg contained 684 healthy volunteers with an age range between 18 and 73 years of age with an average age of 32 and a standard deviation of 14 years. Notably the age distribution recorded at the University of Salzburg was bimodal (with 423 subjects being below 30, the sample does not reflect an age-diverse population; see Supplementary S2). For the ECG data, no specific exclusion criteria for participants was applied. Data from MEG/EEG participants were excluded when no independent heart component equal or above the threshold was found ($r > 0.4$; see MEG/EEG Processing - pre-processing). Furthermore, when the automated processing procedure resulted in errors, data was considered as missing. This resulted in a total of 1104 ECG recordings from PhysioNet, 627 MEG recordings from Cam-CAN and 655 MEG recordings from the University of Salzburg.

Statistical Inference

To investigate the relationship between age and aperiodic activity recorded using MEG, we used bayesian generalized linear models (GLMs) either built directly in PyMC (a python package for probabilistic programming; (Salvatier et al., 2016)) or in Bambi (a high-level interface to PyMC; (Capretto et al., 2022)). Decisions for either Bambi or PyMC were made based on the accessibility of appropriate statistical families for the respective dependent variables in a GLM. Priors were chosen to be weakly informative (exact prior specifications for each model can be obtained from the code in the corresponding authors github repository; see Data and Code availability). Results were considered statistically significant if 94% of the highest (probability) density interval (HDI) of the posterior for a given

standardized β-coefficient or (partial) correlation coefficient was not overlapping with a region of practical equivalence between -0.1 and 0.1 as suggested by Kruschke (2018) based on negligible effect sizes according to Cohen (1988). Furthermore, it was ensured that for all models there were no divergent transitions ($R_{hat} < 1.05$ for all relevant parameters) and an effective sample size > 400 (an exhaustive summary of bayesian model diagnostics can be found in (Vehtari et al., 2021)).

MEG/EEG Processing

MEG/EEG Processing - Data acquisition

MEG data (Cam-CAN; Figure 1ABCD, 2, 3 & 4) was recorded at the University of Cambridge, using a 306 VectorView system (Elekta Neuromag, Helsinki). MEG data (Salzburg; Figure 1 & Supplementary S3) was recorded at the University of Salzburg, using a 306 channel TRIUX system (MEGIN Oy, Helsinki). Both systems are equipped with 102 magnetometers and 204 planar gradiometers and positioned in magnetically shielded rooms. In order to facilitate offline artifact correction, electrooculogram (VEOG, HEOG) as well as ECG was measured continuously in both recording sites. In a subset of the Salzburg recordings EEG was measured additionally (see Figure 1EFGH) using a 32-channel system provided by the MEG manufacturer. Data recorded at Cambridge was online filtered at 0.03-330 Hz, whereas data recorded at Salzburg was online filtered at 0.1-333 Hz with a 1000 Hz sampling rate at both recording sites. Five Head-Position Indicator coils were used to measure the position of the head. All data used in the present study contains passive resting-state measurements lasting about ~8min (Cambridge) and ~5min (Salzburg). Further data processing at both recording sites was conducted similarly and will therefore be reported together.

MEG/EEG Processing - pre-processing

Initially, a Signal-Space-Separation (SSS; (Taulu & Kajola, 2005; Taulu & Simola, 2006)) algorithm was used to find and repair bad channels (implemented in MNE-Python *version 1.2*; (Gramfort, 2013)). The data was further processed by either not applying further SSS cleaning (main manuscript) or by applying an SSS algorithm for additional data cleaning (Supplementary 4/6; implemented in MNE-Python *version 1.2*; (Gramfort, 2013)). The data were afterwards high-pass filtered at 0.1Hz using a finite impulse response (FIR) filter (Hamming window). EEG data was re-referenced to the common average (common practice

in the field; see (Yao et al., 2019)). For extracting physiological "artifacts" from the data, 50 independent components were calculated using the *fastica* algorithm ((Hyvarinen, 1999); implemented in MNE-Python *version 1.2*; note: 50 components were selected for MEG for computational reasons for the analysis of EEG data no threshold was applied). As ICA is sensitive to low-frequency drifts, independent components were calculated on a copy of the data high-pass filtered at 1Hz. Components related to cardiac and ocular activity were determined via correlation with concurrent ECG, VEOG and HEOG recordings. A threshold of $r > 0.4$ was applied to detect the ECG components and a threshold $r > 0.8$ for detecting EOG components in the data. The more sensitive threshold used for ECG component detection was decided upon based on the strong presence of ECG signals in resting state M/EEG recordings (see Figure 1EFGH). The computed ICA was then applied to the original data, either rejecting all components apart from those related to the ECG, or rejecting only EOG related components, or ECG and EOG related components. This resulted in three conditions $MEG_{ECG\ not\ rejected}$, $MEG_{ECG\ rejected}$ and $MEG_{ECG\ component}$. The data were then split into 2 second epochs and residual artifacts were determined using an adaptive and automatic artifact detection method (the "Riemannian Potato" implemented in pyriemann; (Barachant et al., 2013)). Epochs were rejected when the covariance matrix of an epoch differed by >2.5 standard deviations from a centroid covariance matrix.

MEG/EEG Processing - Temporal Response Functions

To estimate the extent at which ECG activity is captured by MEG/EEG recordings, we calculated temporal response functions (TRFs). In brief, the assumption behind a TRF is that a dependent variable is the result of one (or several) predictor variables. This approach can be used to model a time-series as a linear function of one (or several) time series and can be formulated (for a single predictor; see (Brodbeck et al., 2021)) as:

$$y_t = \sum_{\tau=\tau_{min}}^{\tau_{max}} h_\tau x_{t-\tau}$$

Where h represents the TRF, sometimes described as filter kernel, and τ represents potential delays between y and x (for an extensive explanation of the algorithm used herein see (Brodbeck et al., 2021)). Typically, this approach is used to estimate spectro-temporal receptive fields, e.g. in response to auditory stimuli (David et al., 2007), where the

interpretation of a TRF follows that of an ERP/F in response to a continuous input signal (Lalor et al., 2006). This model can be used as a forward or encoding model to predict the brain response from a stimulus representation or as a backward or decoding model to reconstruct a stimulus representation from brain recordings. We used this approach here to detect whether ECG and M/EEG influence each other. Forward and Backward models were calculated between the M/EEG signal and the signal recorded using ECG. This was done to see if signals measured using M/EEG and ECG follow/precede each other (non zero-time lags; e.g. via interoception see (Schulz, 2016)) or if the signals are instantaneously related (zero-time-lags; therefore likely corresponding to the same underlying signal source). As computations of TRFs are memory and time extensive, the MEG, EEG and ECG data were additionally low pass filtered at 45Hz (to avoid aliasing) and downsampled to 100Hz before the analysis (a common practice when computing TRFs; see (Brodbeck et al., 2021)). The TRF time courses visualized in Figure 1E were obtained by computing a principle component analysis (PCA; (Pearson, 1901)) within subject and across all channels, whereas the distribution of peaks visualized in Figure 1F was obtained by calculating the RMS across channels and extracting the maximum value.

MEG/EEG Processing - Spectral analysis

Power spectra were computed using Welch's method (Welch, 1967) between 0.1 and 145Hz (0.5 Hz resolution). Aperiodic activity was extracted using the IRASA method (Wen & Liu, 2016) implemented in the YASA package (Vallat & Walker, 2021). Furthermore, in addition to the main model fit between 0.1-145Hz, additional slopes were fitted to the aperiodic spectrum in 5Hz steps starting from 45Hz as upper frequency limit and in 1Hz steps from 0.5Hz to 10Hz as lower frequency limit. Additionally, to investigate the robustness of our result the spectral parameterization algorithm (implemented in *FOOOF* version 1.0.0; (Donoghue et al., 2020)) was used to parametrize raw power spectra. Power spectra were parameterized across frequency ranges of 0.5–145 Hz. FOOOF models were fit using the following settings: peak width limits: [1 – 6]; max number of peaks: 2; minimum peak height: 0.0; peak threshold: 2.0; aperiodic mode: ‘fixed’. Goodness of fit metrics for both IRASA and FOOOF can be found in Supplementary S1.

ECG Processing

The ECG data recorded as part of the MEG recordings were processed alongside the MEG data. Therefore the pre-processing and spectral analysis settings from the section "MEG/EEG Processing" also apply to the ECG aspect of datasets 3 & 4 (see Figure 1). Below, ECG processing for the data obtained from PhysioNet are described.

ECG Processing - Data acquisition

The ECG data obtained from PhysioNet were acquired at the Jena university hospital (Schumann & Bär, 2021). The study was approved by the ethics committee of the Medical Faculty of the Friedrich Schiller University Jena. All research was performed in accordance with relevant guidelines and regulations. The informed written consent was obtained from all subjects. ECG data were recorded at a sampling rate of 1000 Hz using one of two different recording devices. Either an MP150 (ECG100C, BIOPAC systems inc., Golata, CA, USA) or a Task Force Monitor system (CNSystems Medizintechnik GmbH, Graz AUT). More detailed information about the ECG recordings can be obtained from https://physionet.org/content/autonomic-aging-cardiovascular/1.0.0/. The data were further analyzed using spectral analysis.

ECG Processing - Spectral analysis

Power spectra were computed using Welch's method (Welch, 1967) implemented in *neurodsp* (Cole et al., 2019) between 0.1 and 145Hz (0.5 Hz resolution). The spectral parameterization algorithm (implemented in *FOOOF* version 1.0.0; (Donoghue et al., 2020)) was then used to parametrize the power spectra. Power spectra were parameterized across a frequency range of 0.5–145 Hz using the same settings specified in "MEG/EEG Processing - Spectral analysis"). However, the aperiodic mode was set to 'knee' given that the power spectra (on average) showed a clear 'knee' in log-log coordinates (see Figure 1A).

Data and Code availability

The data analyzed in the main manuscript are mostly obtained from open data sources. The ECG data (Dataset 1 & 2; Figure 1) were obtained from https://physionet.org/content/autonomic-aging-cardiovascular/1.0.0. The MEG/EEG dataset (Figure 1) was obtained at the University of Salzburg as part of routine resting state MEG recordings and is available upon request. The data for the MEG analysis in the main

manuscript (Figure 2 & 3) are obtained from the Cam-CAN repository https://www.cam-can.org/index.php?content=functional. All code used for the analysis is publicly available on GitHub at https://github.com/schmidtfa/cardiac_1_f.

Acknowledgements

The authors thank Freek van Ede, Tzvetan Popov, Rik Henson and Kamen Tsvetanov for helpful comments and discussions and Thomas Hartmann for a code review. Sarah K. Danböck was supported by the Doctoral College 'Imaging the Mind' of the Austrian Science Fund (FWF; W1233-B; Subproject Principal Investigator: Frank H. Wilhelm). No specific funding was acquired for this project. The authors declare no conflicts of interest.

Author contributions

Conceptualization: FS, NW

Formal Analysis: FS, SKD

Investigation: FS

Methodology: FS, GD

Software: FS

Supervision: NW, GD

Visualization: FS

Writing—original draft: FS

Writing—review & editing: FS, SKD, ET, NW, GD

SUPPLEMENTARY MATERIAL

Supplementary S1 - Raw Spectra + Goodness of fit metrics:

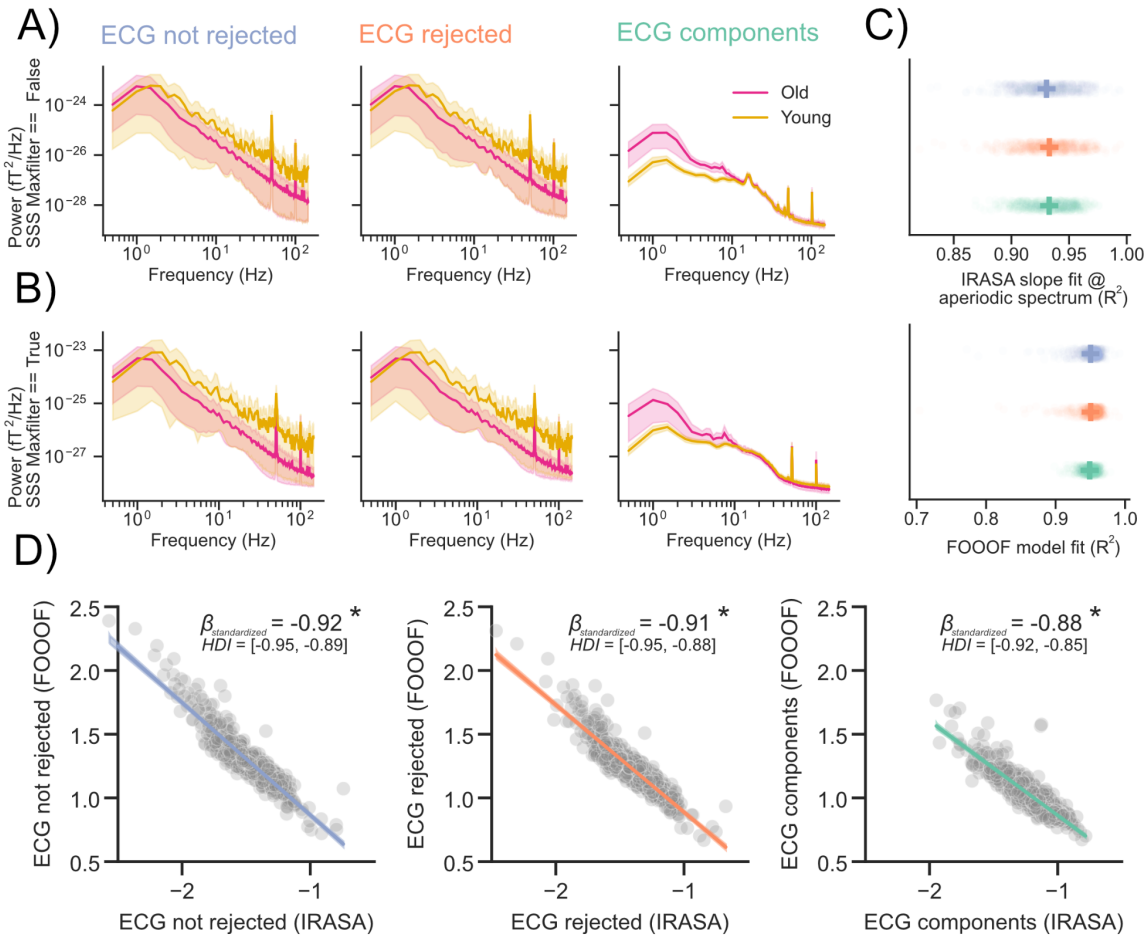

Supplementary S1: Grand average power spectra for the MEG data recorded at Cambridge and split in the three conditions $MEG_{ECG\ not\ rejected}$, $MEG_{ECG\ rejected}$, $MEG_{ECG\ components}$. **A)** Spectra averaged across channels split in older and younger subjects (median split). **B)** Aperiodic activity was extracted from the power spectra using the IRASA method (Wen & Liu, 2016) implemented in the YASA package (Vallat & Walker, 2021). * indicate a “significant” effect (see Methods - Statistical Inference).

Supplementary S2 - Replication FOOOF:

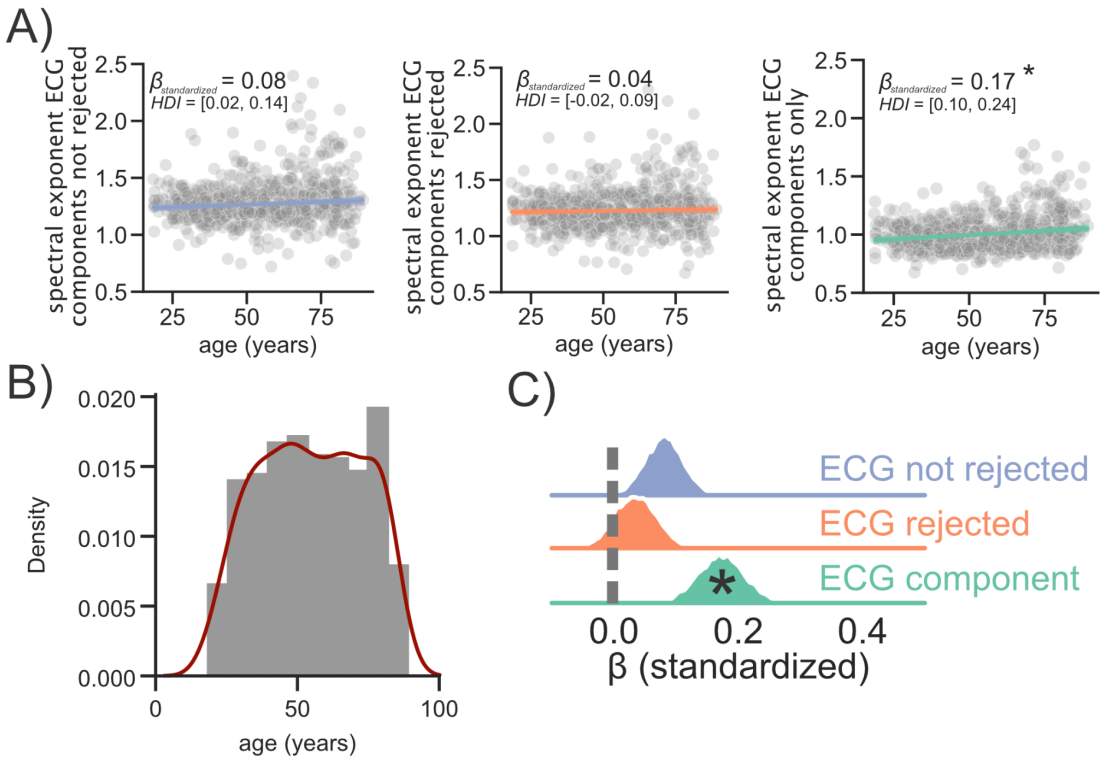

Figure 2: Age-related changes in aperiodic brain activity can be explained by cardiac components **A)** Age was used to predict the spectral exponent at rest in three different conditions (ECG components not rejected [blue], ECG components rejected [orange], ECG components only [green]. **B)** Age distribution in the sample recorded at the University of Cambridge. **C)** Comparison of standardized beta coefficients shows that the strongest association with age is present on the data reflecting only ECG components. * indicate a "significant" effect (see Methods - Statistical Inference).

Supplementary S3 - Replication Salzburg Sample:

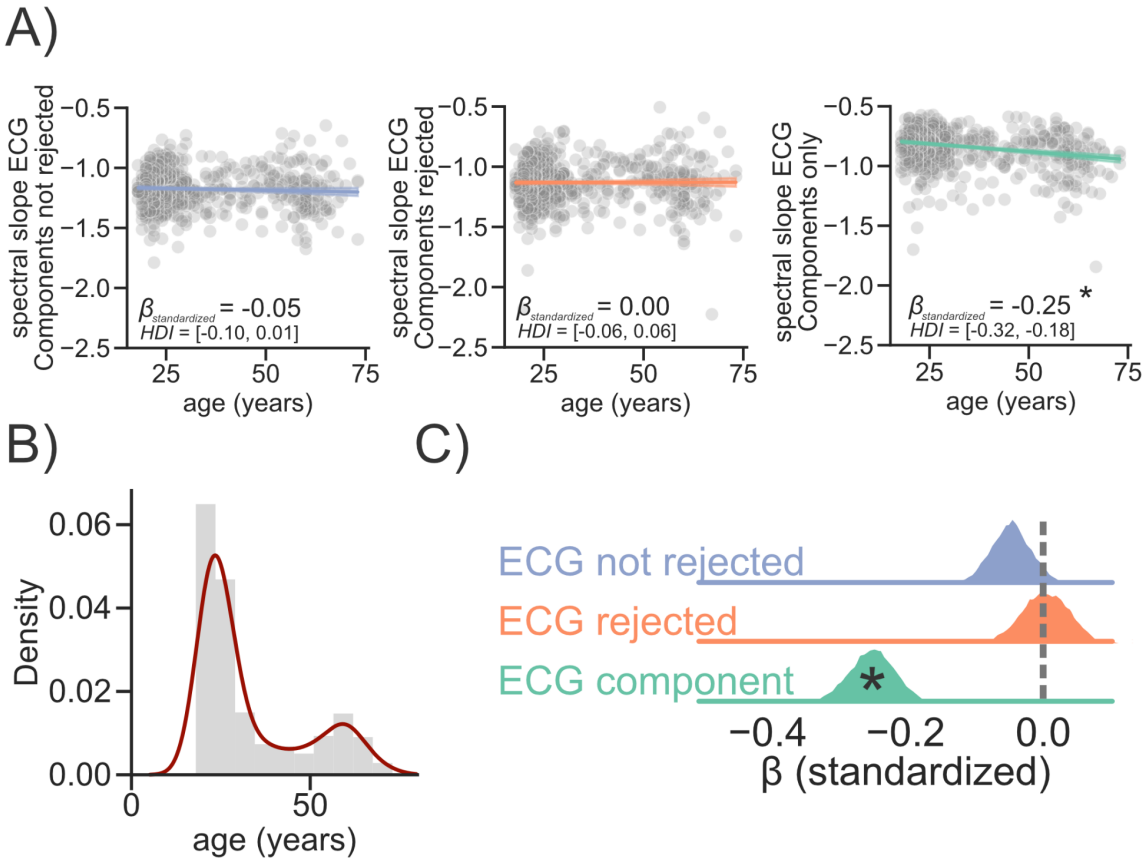

Supplementary S3: Age-related changes in aperiodic brain activity can be explained by cardiac components **A)** Age was used to predict the spectral exponent at rest in three different conditions (ECG components not rejected [blue], ECG components rejected [orange], ECG components only [green]. **B)** Age distribution in the sample routinely recorded as part of MEG measurements at the University of Salzburg. **C)** Comparison of standardized beta coefficients shows that the strongest association with age is present on the data reflecting only ECG components * indicate a "significant" effect (see Methods - Statistical Inference).

Supplementary S4 - SSS Maxfilter Analysis:

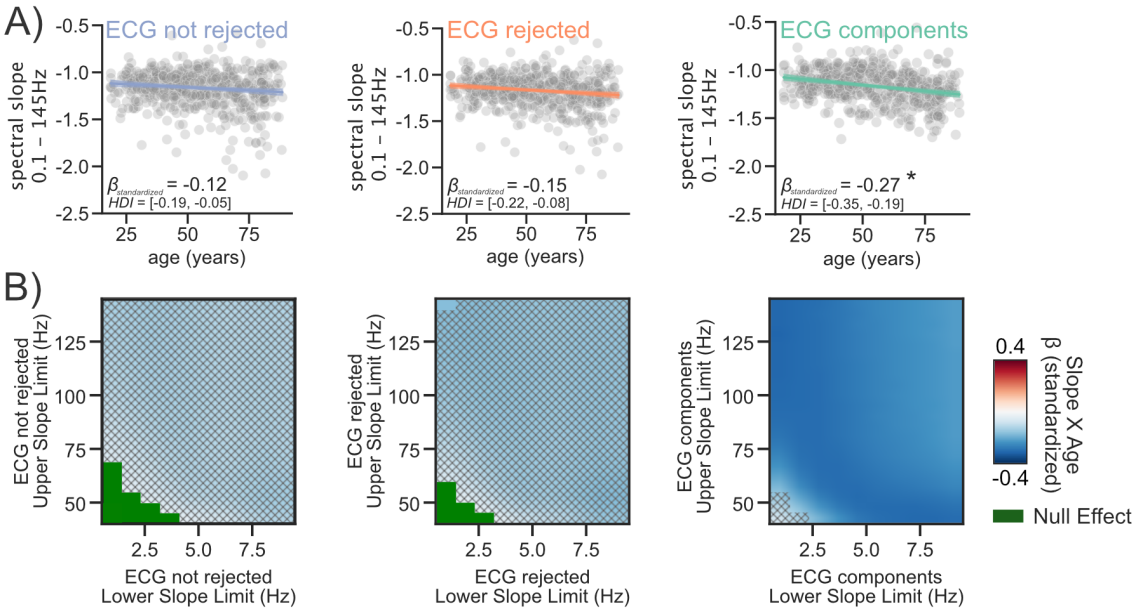

Supplementary S4: SSS Maxfilter Analysis: Age-related changes in aperiodic brain activity are explained by cardiac components **A)** Age was used to predict the spectral slope (fitted at 0.1-145Hz) at rest in three different conditions (ECG components not rejected [blue], ECG components rejected [orange], ECG components only [green]. **B)** The analysis in **A)** was repeated for different fitting ranges with lower limits starting at 0.5 Hz in 1Hz steps ranging until 10 Hz and upper limits starting at 45 Hz in 5 Hz steps ranging until 145 Hz. Significant effects, i.e. effects with credible intervals not overlapping with a region of practical equivalence (ROPE; see Methods - Statistical Inference), are highlighted in red or blue (see colorbar). Null effects, which were defined as effects with credible intervals completely within a ROPE, are highlighted in green. Results where no decision to accept or reject (see (Kruschke, 2018)) an effect could be made, are masked using hatches.

Supplementary S5 - ICA Thresholds:

Table 1: age-related changes in spectral slope (using different ICA thresholds)

	$\beta_{standardized}$	hdi 3%	hdi 97%
ICA Threshold $r > 0.4$ ($N = 627$)			
$MEG_{ECG\ not\ rejected} \sim 1 + age$	-0.168*	-0.235	-0.102
$MEG_{ECG\ rejected} \sim 1 + age$	-0.084	-0.163	-0.013
$MEG_{ECG\ component} \sim 1 + age$	-0.313*	-0.387	-0.244
ICA Threshold $r > 0.5$ ($N = 597$)			
$MEG_{ECG\ not\ rejected} \sim 1 + age$	-0.178*	-0.250	-0.120
$MEG_{ECG\ rejected} \sim 1 + age$	-0.097	-0.172	-0.022
$MEG_{ECG\ component} \sim 1 + age$	-0.304*	-0.379	-0.231
ICA Threshold $r > 0.6$ ($N = 537$)			
$MEG_{ECG\ not\ rejected} \sim 1 + age$	-0.166	-0.242	-0.088
$MEG_{ECG\ rejected} \sim 1 + age$	-0.089	-0.167	-0.011
$MEG_{ECG\ component} \sim 1 + age$	-0.290*	-0.365	-0.210
ICA Threshold $r > 0.7$ ($N = 468$)			
$MEG_{ECG\ not\ rejected} \sim 1 + age$	-0.151	-0.232	-0.067
$MEG_{ECG\ rejected} \sim 1 + age$	-0.072	-0.156	0.015
$MEG_{ECG\ component} \sim 1 + age$	-0.278*	-0.362	-0.195
ICA Threshold $r > 0.8$ ($N = 278$)			
$MEG_{ECG\ not\ rejected} \sim 1 + age$	-0.131	-0.240	-0.025
$MEG_{ECG\ rejected} \sim 1 + age$	-0.068	-0.175	0.041
$MEG_{ECG\ component} \sim 1 + age$	-0.292*	-0.395	-0.176

Note: Dependent Variable = spectral slope; * indicate “significant” effects (see Methods - Statistical Inference)

Supplementary S6 - SSS Maxfilter Analysis:

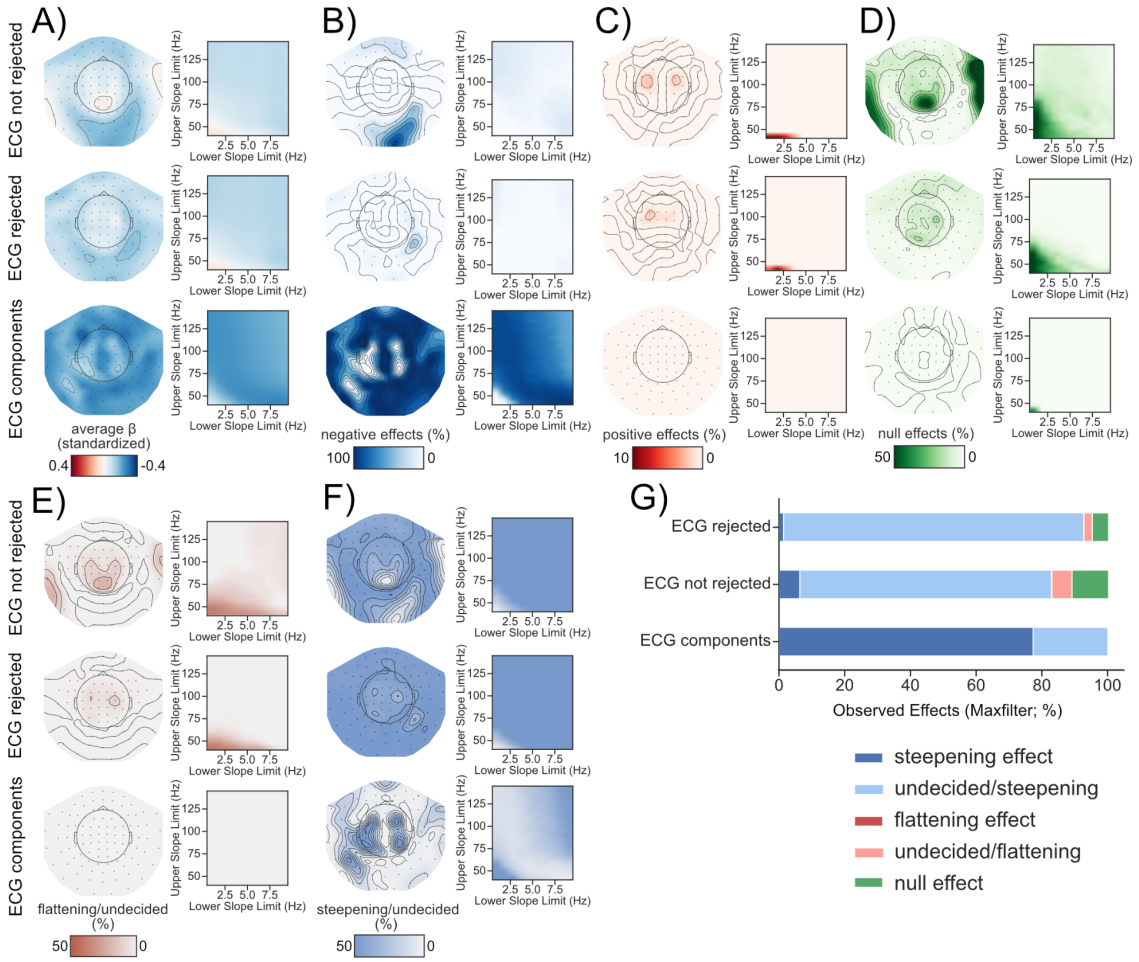

Supplementary S6: SSS Maxfilter Analysis: Steepening and flattening of the spectral slope with age is dependent on the sensor location and the investigated frequency range. Age was used to predict the spectral slope at rest in three different conditions (ECG components not rejected, ECG components rejected and ECG components only) per channel across a variety of frequency ranges (see Figure **1B**). **A)** Standardized beta coefficients either per channel averaged across all frequency ranges (left) or per frequency range (right) averaged across all channels. Age-related **B)** steepening, **C)** flattening and **D)** null effects in the spectral slope were observed and visualized in a similar manner as in **A)**. **EF)** We further show the direction of results where we didn't find enough evidence to support either a steepening, flattening or null effect. **G)** Summary of all observed findings in %.

Supplementary S7 - Head Movement, EOG control analysis:

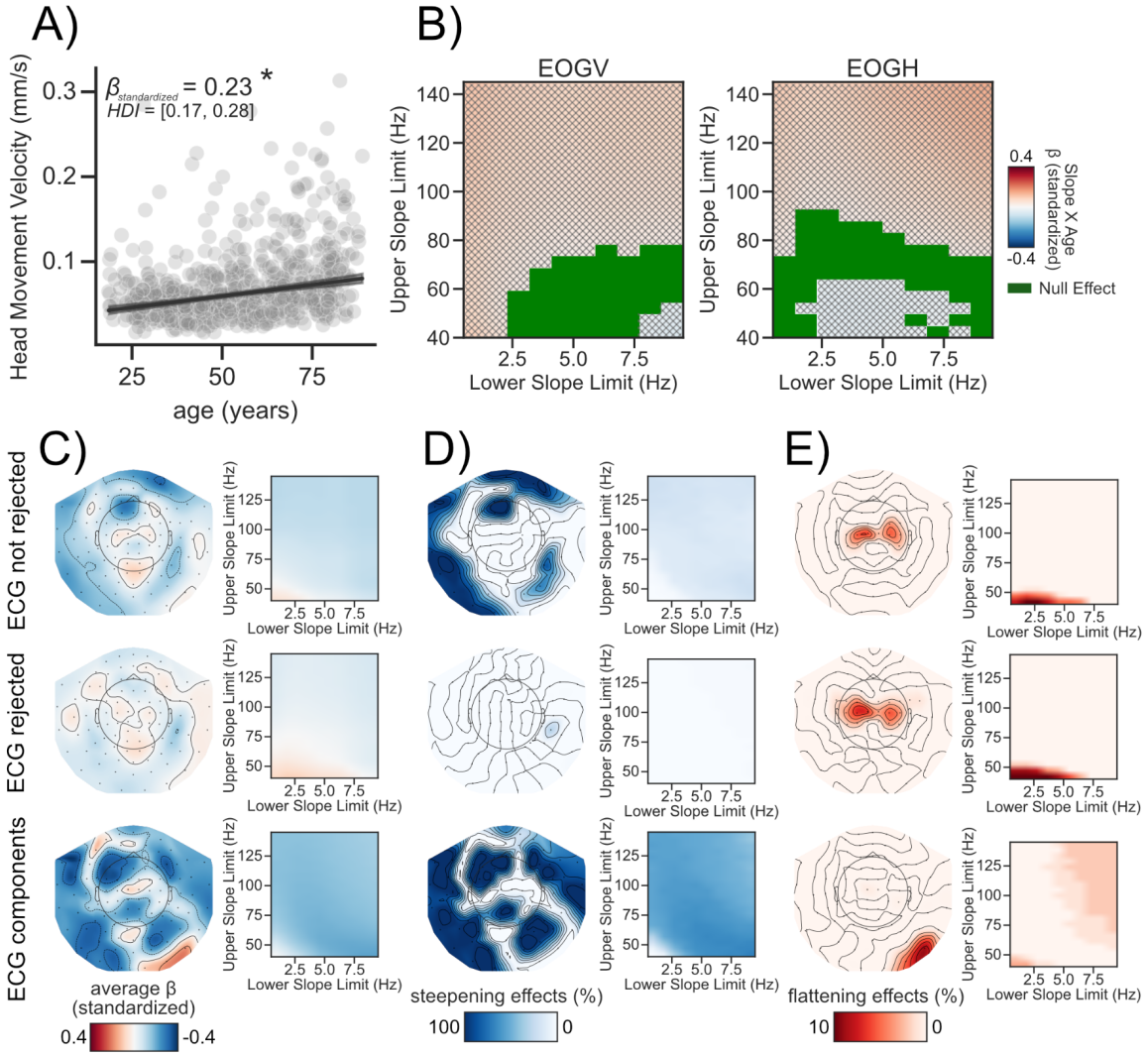

Supplementary S7: Steepening and flattening of the spectral slope with age is dependent on the recording site and the investigated frequency range, when controlling for head movements. **A)** Head movement velocity was estimated using information obtained from the cHPI measurement. **B)** Spectral slopes were obtained also for horizontal and vertical EOG electrodes on the same frequency ranges as in **Figure 2B**. Age was used to predict the spectral slope at rest in three different conditions (ECG components not rejected, ECG components rejected and ECG components only) per channel across a variety of frequency ranges (see Figure **1B**). **C)** Standardized beta coefficients either per channel averaged across all frequency ranges (left) or per frequency range (right) averaged across all channels. Age-related **D)** steepening, **E)** flattening. Significant effects, i.e. effects with credible intervals not overlapping with a region of practical equivalence (ROPE; see Methods - Statistical Inference), are highlighted in red or blue (see colorbar). Null effects, which were defined as effects with credible intervals completely within a ROPE, are highlighted in green. Results where no decision to accept or reject (see (Kruschke, 2018)) an effect could be made, are masked using hatches.

REFERENCES

Ansakorpi, H. (2002). Heart rate dynamics in refractory and well controlled temporal lobe epilepsy. *Journal of Neurology, Neurosurgery & Psychiatry*, *72*(1), 26–30. https://doi.org/10.1136/jnnp.72.1.26

Azuaje, F., Clifford, G., & McSharry, P. (2006). *Advanced Methods and Tools for ECG Data Analysis*. Artech.

Bak, P., Tang, C., & Wiesenfeld, K. (1987). Self-organized criticality: An explanation of the 1/*f* noise. *Physical Review Letters*, *59*(4), 381–384. https://doi.org/10.1103/PhysRevLett.59.381

Barachant, A., Andreev, A., & Congedo, M. (2013). The Riemannian Potato: An automatic and adaptive artifact detection method for online experiments using Riemannian geometry. *TOBI Workshop VI*, 19–20. https://doi.org/hal-00781701

Beckers, F., Verheyden, B., & Aubert, A. E. (2006). Aging and nonlinear heart rate control in a healthy population. *American Journal of Physiology-Heart and Circulatory Physiology*, *290*(6), H2560–H2570. https://doi.org/10.1152/ajpheart.00903.2005

Bedard, C., Gomes, J.-M., Bal, T., & Destexhe, A. (2017). A framework to reconcile frequency scaling measurements, from intracellular recordings, local-field potentials, up to EEG and MEG signals. *Journal of Integrative Neuroscience*, *16*(1), 3–18. https://doi.org/10.3233/JIN-160001

Bedard, C., Piette, C., Venance, L., & Destexhe, A. (2022). Extracellular and intracellular components of the impedance of neural tissue. *Biophysical Journal*, *121*(6), 869–885. https://doi.org/10.1016/j.bpj.2022.02.022

Bénar, C. . G., Grova, C., Jirsa, V. K., & Lina, J. M. (2019). Differences in MEG and EEG power-law scaling explained by a coupling between spatial coherence and frequency: A simulation study. *Journal of Computational Neuroscience*, *47*(1), 31–41.

https://doi.org/10.1007/s10827-019-00721-9

Brodbeck, C., Das, P., Kulasingham, J. P., Bhattasali, S., Gaston, P., Resnik, P., & Simon, J. Z. (2021). *Eelbrain: A Python toolkit for time-continuous analysis with temporal response functions* [Preprint]. Neuroscience. https://doi.org/10.1101/2021.08.01.454687

Buzsáki, G. (2006). *Rhythms of the Brain*. Oxford University Press. https://doi.org/10.1093/acprof:oso/9780195301069.001.0001

Capretto, T., Piho, C., Kumar, R., Westfall, J., Yarkoni, T., & Martin, O. A. (2022). *Bambi: A simple interface for fitting Bayesian linear models in Python* (arXiv:2012.10754). arXiv. http://arxiv.org/abs/2012.10754

Chen, Y.-P., Schmidt, F., Keitel, A., Rösch, S., Hauswald, A., & Weisz, N. (2023). Speech intelligibility changes the temporal evolution of neural speech tracking. *NeuroImage*, *268*, 119894. https://doi.org/10.1016/j.neuroimage.2023.119894

Cohen, J. (1988). *Statistical Power Analysis for the Behavioral Sciences* (0 ed.). Routledge. https://doi.org/10.4324/9780203771587

Cole, S., Donoghue, T., Gao, R., & Voytek, B. (2019). NeuroDSP: A package for neural digital signal processing. *Journal of Open Source Software*, *4*(36), 1272. https://doi.org/10.21105/joss.01272

David, S. V., Mesgarani, N., & Shamma, S. A. (2007). Estimating sparse spectro-temporal receptive fields with natural stimuli. *Network: Computation in Neural Systems*, *18*(3), 191–212. https://doi.org/10.1080/09548980701609235

Deery, H. A., Di Paolo, R., Moran, C., Egan, G. F., & Jamadar, S. D. (2023). The older adult brain is less modular, more integrated, and less efficient at rest: A systematic review of large-scale resting-state functional brain networks in aging. *Psychophysiology*, *60*(1). https://doi.org/10.1111/psyp.14159

Dehghani, N., Bédard, C., Cash, S. S., Halgren, E., & Destexhe, A. (2010). Comparative power spectral analysis of simultaneous elecroencephalographic and magnetoencephalographic recordings in humans suggests non-resistive extracellular media. *Journal of Computational Neuroscience*, *29*(3), 405–421. https://doi.org/10.1007/s10827-010-0263-2

Demanuele, C., James, C. J., & Sonuga-Barke, E. J. (2007). Distinguishing low frequency oscillations within the 1/f spectral behaviour of electromagnetic brain signals. *Behavioral and Brain Functions*, *3*(1), 62. https://doi.org/10.1186/1744-9081-3-62

Dirlich, G., Vogl, L., Plaschke, M., & Strian, F. (1997). Cardiac field effects on the EEG. *Electroencephalography and Clinical Neurophysiology*, *102*(4), 307–315. https://doi.org/10.1016/S0013-4694(96)96506-2

Donoghue, T., Haller, M., Peterson, E. J., Varma, P., Sebastian, P., Gao, R., Noto, T., Lara, A. H., Wallis, J. D., Knight, R. T., Shestyuk, A., & Voytek, B. (2020). Parameterizing neural power spectra into periodic and aperiodic components. *Nature Neuroscience*, *23*(12), 1655–1665. https://doi.org/10.1038/s41593-020-00744-x

Feindel, W., Leblanc, R., & de Almeida, A. N. (2009). Epilepsy Surgery: Historical Highlights 1909-2009. *Epilepsia*, *50*, 131–151. https://doi.org/10.1111/j.1528-1167.2009.02043.x

Gao, R., Peterson, E. J., & Voytek, B. (2017). Inferring synaptic excitation/inhibition balance from field potentials. *NeuroImage*, *158*, 70–78. https://doi.org/10.1016/j.neuroimage.2017.06.078

Gao, R., van den Brink, R. L., Pfeffer, T., & Voytek, B. (2020). Neuronal timescales are functionally dynamic and shaped by cortical microarchitecture. *ELife*, *9*, e61277. https://doi.org/10.7554/eLife.61277

Ghinda, D. C., Lambert, B., Lu, J., Jiang, N., Tsai, E., Sachs, A., Wu, J.-S., & Northoff, G.

(2021). Scale-Free Analysis of Intraoperative ECoG During Awake Craniotomy for Glioma. *Frontiers in Oncology*, *10*, 625474. https://doi.org/10.3389/fonc.2020.625474

Gisiger, T. (2001). Scale invariance in biology: Coincidence or footprint of a universal mechanism? *Biological Reviews of the Cambridge Philosophical Society*, *76*(2), 161–209. https://doi.org/10.1017/S1464793101005607

Goddard, K., Sampson, C., Bedy, S.-M., Ghadban, R., & Stilley, J. (2021). Effect of Ketamine on Cardiovascular Function During Procedural Sedation of Adults. *Cureus*. https://doi.org/10.7759/cureus.14228

Goldberger, A. L., Amaral, L. A. N., Glass, L., Hausdorff, J. M., Ivanov, P. Ch., Mark, R. G., Mietus, J. E., Moody, G. B., Peng, C.-K., & Stanley, H. E. (2000). PhysioBank, PhysioToolkit, and PhysioNet: Components of a New Research Resource for Complex Physiologic Signals. *Circulation*, *101*(23). https://doi.org/10.1161/01.CIR.101.23.e215

Gomes, J.-M., Bédard, C., Valtcheva, S., Nelson, M., Khokhlova, V., Pouget, P., Venance, L., Bal, T., & Destexhe, A. (2016). Intracellular Impedance Measurements Reveal Non-ohmic Properties of the Extracellular Medium around Neurons. *Biophysical Journal*, *110*(1), 234–246. https://doi.org/10.1016/j.bpj.2015.11.019

Gramfort, A. (2013). MEG and EEG data analysis with MNE-Python. *Frontiers in Neuroscience*, *7*. https://doi.org/10.3389/fnins.2013.00267

Gross, J., Baillet, S., Barnes, G. R., Henson, R. N., Hillebrand, A., Jensen, O., Jerbi, K., Litvak, V., Maess, B., Oostenveld, R., Parkkonen, L., Taylor, J. R., van Wassenhove, V., Wibral, M., & Schoffelen, J.-M. (2013). Good practice for conducting and reporting MEG research. *NeuroImage*, *65*, 349–363. https://doi.org/10.1016/j.neuroimage.2012.10.001

Haapaniemi, T. H. (2001). Ambulatory ECG and analysis of heart rate variability in Parkinson's disease. *Journal of Neurology, Neurosurgery & Psychiatry*, *70*(3), 305–310. https://doi.org/10.1136/jnnp.70.3.305

Haenschel, C., Bittner, R. A., Haertling, F., Rotarska-Jagiela, A., Maurer, K., Singer, W., & Linden, D. E. J. (2007). Contribution of Impaired Early-Stage Visual Processing to Working Memory Dysfunction in Adolescents With Schizophrenia: A Study With Event-Related Potentials and Functional Magnetic Resonance Imaging. *Archives of General Psychiatry*, *64*(11), 1229. https://doi.org/10.1001/archpsyc.64.11.1229

He, B. J., Zempel, J. M., Snyder, A. Z., & Raichle, M. E. (2010). The Temporal Structures and Functional Significance of Scale-free Brain Activity. *Neuron*, *66*(3), 353–369. https://doi.org/10.1016/j.neuron.2010.04.020

He, W., Donoghue, T., Sowman, P. F., Seymour, R. A., Brock, J., Crain, S., Voytek, B., & Hillebrand, A. (2019). *Co-Increasing Neuronal Noise and Beta Power in the Developing Brain* [Preprint]. Neuroscience. https://doi.org/10.1101/839258

Hunt, A. C. (2002). T Wave Alternans in high arrhythmic risk patients: Analysis in time and frequency domains: A pilot study. *BMC Cardiovascular Disorders*, *2*(1), 6. https://doi.org/10.1186/1471-2261-2-6

Hyvarinen, A. (1999). Fast and robust fixed-point algorithms for independent component analysis. *IEEE Transactions on Neural Networks*, *10*(3), 626–634. https://doi.org/10.1109/72.761722

Jousmäki, V., & Hari, R. (1996). Cardiac Artifacts in Magnetoencephalogram: *Journal of Clinical Neurophysiology*, *13*(2), 172–176. https://doi.org/10.1097/00004691-199603000-00008

Kanaya, N., Hirata, N., Kurosawa, S., Nakayama, M., & Namiki, A. (2003). Differential Effects of Propofol and Sevoflurane on Heart Rate Variability. *Anesthesiology*, *98*(1), 34–40.

https://doi.org/10.1097/00000542-200301000-00009

Kern, M., Aertsen, A., Schulze-Bonhage, A., & Ball, T. (2013). Heart cycle-related effects on event-related potentials, spectral power changes, and connectivity patterns in the human ECoG. *NeuroImage*, *81*, 178–190. https://doi.org/10.1016/j.neuroimage.2013.05.042

Kozhemiako, N., Mylonas, D., Pan, J. Q., Prerau, M. J., Redline, S., & Purcell, S. M. (2022). Sources of Variation in the Spectral Slope of the Sleep EEG. *Eneuro*, *9*(5), ENEURO.0094-22.2022. https://doi.org/10.1523/ENEURO.0094-22.2022

Kruschke, J. K. (2018). Rejecting or Accepting Parameter Values in Bayesian Estimation. *Advances in Methods and Practices in Psychological Science*, *1*(2), 270–280. https://doi.org/10.1177/2515245918771304

Lalor, E. C., Pearlmutter, B. A., Reilly, R. B., McDarby, G., & Foxe, J. J. (2006). The VESPA: A method for the rapid estimation of a visual evoked potential. *NeuroImage*, *32*(4), 1549–1561. https://doi.org/10.1016/j.neuroimage.2006.05.054

Lendner, J. D., Helfrich, R. F., Mander, B. A., Romundstad, L., Lin, J. J., Walker, M. P., Larsson, P. G., & Knight, R. T. (2020). An electrophysiological marker of arousal level in humans. *ELife*, *9*, e55092. https://doi.org/10.7554/eLife.55092

Merkin, A., Sghirripa, S., Graetz, L., Smith, A. E., Hordacre, B., Harris, R., Pitcher, J., Semmler, J., Rogasch, N. C., & Goldsworthy, M. (2022). Do age-related differences in aperiodic neural activity explain differences in resting EEG alpha? *Neurobiology of Aging*, S0197458022002019. https://doi.org/10.1016/j.neurobiolaging.2022.09.003

Miller, K. J., Sorensen, L. B., Ojemann, J. G., & den Nijs, M. (2009). Power-Law Scaling in the Brain Surface Electric Potential. *PLoS Computational Biology*, *5*(12), e1000609. https://doi.org/10.1371/journal.pcbi.1000609

Mitra, P. P., & Pesaran, B. (1999). Analysis of Dynamic Brain Imaging Data. *Biophysical*

Journal, *76*(2), 691–708. https://doi.org/10.1016/S0006-3495(99)77236-X

Mohammed, B., Bialkowski, K., Abbosh, A., Mills, P. C., & Bradley, A. P. (2017). Closed-form equation to estimate the dielectric properties of biological tissues as a function of age: Dielectric Properties of Biological Tissues. *Bioelectromagnetics*, *38*(6), 474–481. https://doi.org/10.1002/bem.22054

Mostile, G., Giuliano, L., Dibilio, V., Luca, A., Cicero, C. E., Sofia, V., Nicoletti, A., & Zappia, M. (2019). Complexity of electrocortical activity as potential biomarker in untreated Parkinson's disease. *Journal of Neural Transmission*, *126*(2), 167–172. https://doi.org/10.1007/s00702-018-1961-6

Pearson, K. (1901). LIII. On lines and planes of closest fit to systems of points in space. *The London, Edinburgh, and Dublin Philosophical Magazine and Journal of Science*, *2*(11), 559–572. https://doi.org/10.1080/14786440109462720

Penzel, T., Kantelhardt, J. W., Lo, C.-C., Voigt, K., & Vogelmeier, C. (2003). Dynamics of Heart Rate and Sleep Stages in Normals and Patients with Sleep Apnea. *Neuropsychopharmacology*, *28*(S1), S48–S53. https://doi.org/10.1038/sj.npp.1300146

Pritchard, W. S. (1992). The Brain in Fractal Time: 1/F-Like Power Spectrum Scaling of the Human Electroencephalogram. *International Journal of Neuroscience*, *66*(1–2), 119–129. https://doi.org/10.3109/00207459208999796

Salvatier, J., Wiecki, T. V., & Fonnesbeck, C. (2016). Probabilistic programming in Python using PyMC3. *PeerJ Computer Science*, *2*, e55. https://doi.org/10.7717/peerj-cs.55

Saul, J. P., Albrecht, P., Berger, R. D., & Cohen, R. J. (1988). Analysis of long term heart rate variability: Methods, 1/f scaling and implications. *Computers in Cardiology*, *14*, 419–422.

Schmidt, F., Chen, Y.-P., Keitel, A., Rösch, S., Hannemann, R., Serman, M., Hauswald, A., &

Weisz, N. (2021). *Neural speech tracking shifts from the syllabic to the modulation rate of speech as intelligibility decreases* [Preprint]. Neuroscience. https://doi.org/10.1101/2021.03.25.437033

Schulz, S. M. (2016). Neural correlates of heart-focused interoception: A functional magnetic resonance imaging meta-analysis. *Philosophical Transactions of the Royal Society B: Biological Sciences*, *371*(1708), 20160018. https://doi.org/10.1098/rstb.2016.0018

Schumann, A., & Bär, K. (2021). *Autonomic Aging: A dataset to quantify changes of cardiovascular autonomic function during healthy aging* (1.0.0) [Data set]. PhysioNet. https://doi.org/10.13026/2HSY-T491

Shaffer, F., & Ginsberg, J. P. (2017). An Overview of Heart Rate Variability Metrics and Norms. *Frontiers in Public Health*, *5*, 258. https://doi.org/10.3389/fpubh.2017.00258

Shafto, M. A., Tyler, L. K., Dixon, M., Taylor, J. R., Rowe, J. B., Cusack, R., Calder, A. J., Marslen-Wilson, W. D., Duncan, J., Dalgleish, T., Henson, R. N., Brayne, C., & Matthews, F. E. (2014). The Cambridge Centre for Ageing and Neuroscience (Cam-CAN) study protocol: A cross-sectional, lifespan, multidisciplinary examination of healthy cognitive ageing. *BMC Neurology*, *14*(1), 204. https://doi.org/10.1186/s12883-014-0204-1

Singh, S. (2014). Magnetoencephalography: Basic principles. *Annals of Indian Academy of Neurology*, *17*(5), 107. https://doi.org/10.4103/0972-2327.128676

Takarada-Iemata, M., Westenskow, P. D., & Muramatsu, R. (2019). Neurovascular interaction. *Neurochemistry International*, *129*, 104506. https://doi.org/10.1016/j.neuint.2019.104506

Task Force of the European Society of Cardiology the North American Society of Pacing Electrophysiology. (1996). Heart Rate Variability: Standards of Measurement,

Physiological Interpretation, and Clinical Use. *Circulation*, *93*(5), 1043–1065. https://doi.org/10.1161/01.CIR.93.5.1043

Taulu, S., & Kajola, M. (2005). Presentation of electromagnetic multichannel data: The signal space separation method. *Journal of Applied Physics*, *97*(12), 124905. https://doi.org/10.1063/1.1935742

Taulu, S., & Simola, J. (2006). Spatiotemporal signal space separation method for rejecting nearby interference in MEG measurements. *Physics in Medicine and Biology*, *51*(7), 1759–1768. https://doi.org/10.1088/0031-9155/51/7/008

Taylor, J. R., Williams, N., Cusack, R., Auer, T., Shafto, M. A., Dixon, M., Tyler, L. K., Cam-CAN, & Henson, R. N. (2017). The Cambridge Centre for Ageing and Neuroscience (Cam-CAN) data repository: Structural and functional MRI, MEG, and cognitive data from a cross-sectional adult lifespan sample. *NeuroImage*, *144*, 262–269. https://doi.org/10.1016/j.neuroimage.2015.09.018

Thomas, C., Datta, A., & Woods, A. (2018). Effect of Aging on Cortical Current Flow Due to Transcranial Direct Current Stimulation: Considerations for Safety. *2018 40th Annual International Conference of the IEEE Engineering in Medicine and Biology Society (EMBC)*, 3084–3087. https://doi.org/10.1109/EMBC.2018.8513014

Thuwal, K., Banerjee, A., & Roy, D. (2021). Aperiodic and Periodic Components of Ongoing Oscillatory Brain Dynamics Link Distinct Functional Aspects of Cognition across Adult Lifespan. *Eneuro*, *8*(5), ENEURO.0224-21.2021. https://doi.org/10.1523/ENEURO.0224-21.2021

Tröndle, M., Popov, T., Dziemian, S., & Langer, N. (2022). Decomposing the role of alpha oscillations during brain maturation. *ELife*, *11*, e77571. https://doi.org/10.7554/eLife.77571

Vallat, R., & Walker, M. P. (2021). An open-source, high-performance tool for automated

sleep staging. *ELife*, *10*, e70092. https://doi.org/10.7554/eLife.70092

Vehtari, A., Gelman, A., Simpson, D., Carpenter, B., & Bürkner, P.-C. (2021). Rank-Normalization, Folding, and Localization: An Improved R̂ for Assessing Convergence of MCMC (with Discussion). *Bayesian Analysis*, *16*(2). https://doi.org/10.1214/20-BA1221

von Rosenberg, W., Chanwimalueang, T., Goverdovsky, V., Peters, N. S., Papavassiliou, C., & Mandic, D. P. (2017). Hearables: Feasibility of recording cardiac rhythms from head and in-ear locations. *Royal Society Open Science*, *4*(11), 171214. https://doi.org/10.1098/rsos.171214

Voytek, B., Kramer, M. A., Case, J., Lepage, K. Q., Tempesta, Z. R., Knight, R. T., & Gazzaley, A. (2015). Age-Related Changes in 1/f Neural Electrophysiological Noise. *Journal of Neuroscience*, *35*(38), 13257–13265. https://doi.org/10.1523/JNEUROSCI.2332-14.2015

Waschke, L., Donoghue, T., Fiedler, L., Smith, S., Garrett, D. D., Voytek, B., & Obleser, J. (2021). Modality-specific tracking of attention and sensory statistics in the human electrophysiological spectral exponent. *ELife*, *10*, e70068. https://doi.org/10.7554/eLife.70068

Welch, P. (1967). The use of fast Fourier transform for the estimation of power spectra: A method based on time averaging over short, modified periodograms. *IEEE Transactions on Audio and Electroacoustics*, *15*(2), 70–73. https://doi.org/10.1109/TAU.1967.1161901

Wen, H., & Liu, Z. (2016). Separating Fractal and Oscillatory Components in the Power Spectrum of Neurophysiological Signal. *Brain Topography*, *29*(1), 13–26. https://doi.org/10.1007/s10548-015-0448-0

Yao, D., Qin, Y., Hu, S., Dong, L., Bringas Vega, M. L., & Valdés Sosa, P. A. (2019). Which

Reference Should We Use for EEG and ERP practice? *Brain Topography*, *32*(4), 530–549. https://doi.org/10.1007/s10548-019-00707-x